

Ionized zinc vacancy mediated ferromagnetism in copper doped ZnO thin films

Cite as: AIP Advances 2, 012184 (2012); <https://doi.org/10.1063/1.3698314>

Submitted: 20 December 2011 • Accepted: 25 February 2012 • Published Online: 23 March 2012

Shi-Yi Zhuo, Xue-Chao Liu, Ze Xiong, et al.



View Online



Export Citation

ARTICLES YOU MAY BE INTERESTED IN

[A comprehensive review of ZnO materials and devices](#)

Journal of Applied Physics **98**, 041301 (2005); <https://doi.org/10.1063/1.1992666>

[Room-temperature ferromagnetism in Cu-doped ZnO thin films](#)

Applied Physics Letters **87**, 082504 (2005); <https://doi.org/10.1063/1.2032588>

[Defects in ZnO](#)

Journal of Applied Physics **106**, 071101 (2009); <https://doi.org/10.1063/1.3216464>

AIP Advances
Mathematical Physics Collection

READ NOW

The banner features a dark blue background with a 3D bar chart on the left. The text "AIP Advances" and "Mathematical Physics Collection" is centered in white. A "READ NOW" button is in the bottom right corner.

Ionized zinc vacancy mediated ferromagnetism in copper doped ZnO thin films

Shi-Yi Zhuo,^{1,2} Xue-Chao Liu,^{1,a} Ze Xiong,^{1,2} Jian-Hua Yang,¹ and Er-Wei Shi¹

¹Shanghai Institute of Ceramics, Chinese Academy of Sciences, Shanghai 200050, China

²Graduate University of Chinese Academy of Sciences, Beijing 100049, China

(Received 20 December 2011; accepted 25 February 2012; published online 23 March 2012)

This paper reports the origin of ferromagnetism in Cu-doped ZnO thin films. Room-temperature ferromagnetism is obtained in all the thin films when deposited at different oxygen partial pressure. An obviously enhanced peak corresponding to zinc vacancy is observed in the photoluminescence spectra, while the electrical spin resonance measurement implies the zinc vacancy is negative charged. After excluding the possibility of direct exchange mechanisms (via free carriers), we tentatively propose a quasi-indirect exchange model (via ionized zinc vacancy) for Cu-doped ZnO system. Copyright 2012 Author(s). This article is distributed under a Creative Commons Attribution 3.0 Unported License. [<http://dx.doi.org/10.1063/1.3698314>]

The origin of ferromagnetism in ZnO based diluted magnetic semiconductor (DMS) has attracted intensive attention in the past decade.^{1,2} The bound magnetic polaron (BMP) model reveals that ferromagnetism is mediated via intrinsic point defects, which is thought to be a promising mechanism for defect-rich oxides. Despite significant progress has been achieved, no consensus has been constructed. Hsu *et al.* (Ref. 3) investigated the annealing effect on the magnetism of Co-doped ZnO film and demonstrated that the ferromagnetism was enhanced by oxygen vacancy (V_O). Conversely, Ye *et al.* (Ref. 4) reported that the V_O broke the Cu-O bond, and would be harmful for the ferromagnetism. Hu *et al.* (Ref. 5) reported that the magnetic moment in Cr-doped ZnO films was induced by zinc vacancy (V_{Zn}) on the film surface or at grain boundaries. Moreover, interstitial zinc (Zn_i) was also observed to make contribution to the ferromagnetism.⁶ These controversial results give rise to a question which specific defect is the origin of ferromagnetism in ZnO based DMS? In fact, not all the point defect can form BMPs. In this paper, we only focus on V_{Zn} and V_O which are the most common point defects in ZnO system. The free carriers can be trapped by point defects in ZnO. Therefore, V_O may be in the neutral state (V_O^0 , $s=0$) and/or the positive charge state (V_O^+ , $s=1/2$), while V_{Zn} may be in the neutral state (V_{Zn}^0 , $s=1$) and/or the negative charge state (V_{Zn}^- , $s=1/2$).⁷ Point defect with $s=0$, in which there is no net magnetic moment, will not make contribution to the ferromagnetism.

Cu-doped ZnO thin films have attracted intense attentions in recent years owing to its metallic and oxide compounds (Cu, Cu₂O and CuO) are non-ferromagnetic.⁸ This is considered as an ideal substitution to interpret the origin of ferromagnetism in ZnO based DMS. In this study, a series of Cu-doped ZnO thin films were prepared at different oxygen partial pressure (P_O). The correlation between ionized V_{Zn} and ferromagnetism was studied and discussed based on the characterizations of photoluminescence and electrical spin resonance spectra.

Cu-doped ZnO thin films with nominal composition of 3 at.% were deposited at a series of O₂/Ar mixed atmospheres by an inductively coupled plasma enhanced physical vapor deposition

^aAuthor to whom correspondence should be addressed. Tel.: +86 21 69987663; fax: +86 21 69987661. Electronic mail: xcliu@mail.sic.ac.cn



(ICP-PVD) system. The samples obtained at different P_O of 0 Pa, 0.02 Pa, 0.03 Pa, 0.20 Pa and 0.40 Pa (with total pressure of 1.50 Pa) are marked as S1, S2, S3, S4 and S5 in the following context and figures, respectively. Detailed description of the growth process has been published elsewhere.⁹ The magnetization measurement was performed on a superconducting quantum interference device (SQUID) magnetometer (Quantum Design, MPMS XL-7) at room temperature. The applied magnetic field was parallel to the film surface. The crystalline structure was characterized by a x-ray diffractometer (XRD) with Cu K_α radiation ($\lambda=1.5406 \text{ \AA}$; Rigaku, Ultima IV). The photoluminescence (PL) spectra were investigated on a micro-Raman system with 325 nm wavelength He-Cd excitation laser (Jobin Yvon LabRAM, HR 800UV) at room temperature. The electron spin resonance (ESR) spectra were measured using a spectrometer (JEOL, JES-FA200) at 270 K, operating at X-band frequency of 9.09 GHz with a microwave power of 10.00 mW.

Figure 1(a) shows the magnetization as a function of applied field (M - H) curves of S1, S2, S3, S4 and S5. The diamagnetic contribution from Si substrate has been subtracted from the raw data. The magnetization approaches a saturation value (M_S) when the applied field is increased to ~ 2000 Oe. Clear hysteresis loops are observed in the M - H curves, which reveal obvious room-temperature ferromagnetism in all the thin films. With the increase in P_O , the M_S increases from $0.01 \mu_B/\text{Cu}$ to $0.1 \mu_B/\text{Cu}$. Figure 1(b) illustrates the XRD patterns characterized in the 2θ range from 25° to 65° . A prominent peak corresponding to ZnO (002) with the diffraction angle of 34.62° is observed in all the thin films, while a weak peak (*) corresponding to ZnO (101) at the diffraction angle 36.50° is seen in S1 and S2. The XRD results indicate a preferential orientation characteristic of the Cu-doped ZnO thin films. From the (002) peak, the c -axis lattice length (L_c) can be calculated by the reduced Bragg equation $L_c = \lambda / \sin \theta$, where λ is the x-ray wavelength, θ is the diffraction angle of (002) peak. The L_c is calculated to be 5.18 \AA for all the thin films, which is a little bit smaller than that of undoped ZnO (5.21 \AA). Since the ionic radii of Cu^{1+} , Zn^{2+} and Cu^{2+} are 0.77 \AA , 0.74 \AA and 0.73 \AA , respectively,¹⁰ the XRD result indicates that the most of the Cu dopants are dissolved into the ZnO lattice and shows a chemical valence state of $+2$.

Figure 1(c) shows the PL spectra, in which the frequency-doubled laser related peak (#) at 1.90 eV has been removed. An intense ultraviolet-emission peak at 3.27 eV with a shoulder peak (Δ) at 3.09 eV and an obvious red-emission peak (\blacklozenge) at 1.63 eV are observed. A broad green emission peak (\bullet) at 2.40 eV emerges in S1, but disappears in S2, S3, S4 and S5. The ultraviolet-emission, also known as near band edge emission (NBE), is generally attributed to the exciton transition from the localized level below the conduction band to the valance band. For the broad green emission, Ahan *et al.* (Ref. 11) attributed it to the transition from conductive band to V_O energy level located at 0.9 eV above the valance band. For the shoulder peak, Lin *et al.* (Ref. 12) and Hu *et al.* (Ref. 5) attributed it to the transition from conduction band to V_{Zn} energy level located at 0.3 eV above the valance band. For the red-emission peak, Fang *et al.* (Ref. 13) suggests it is related to a transition from defects under conduct level to V_{Zn} energy level. It can be concluded that the intrinsic point defects in Cu doped ZnO thin films are affected by sputtering atmosphere. With the increase in P_O , the V_O related green emission shows an obvious decrease trend. It is also interesting to mention that with the increase in P_O , the V_{Zn} associated signals, such as the shoulder peak and red-emission peak, are subtly improved.

To characterize the spin polarized ions in the thin films, an in-depth ESR analysis was performed, as shown in Figure 1(d). An obvious Gauss peak at $g=2.0028$ and a weak peak at $g=2.049$ is clearly observed and can be assigned to free carriers ($g=2.0023$) and Cu^{2+} ($g=2.049$) (Ref. 14), respectively. It should be noted that a peak (\square) at $g=1.96$ which is often attributed to the shallow donor state (Ref. 15), is absent in our result. The peak at $g \approx 2.012$ ascribed to V_{Zn}^- ($g_{\parallel} = 2.014$, $g_{\perp} = 2.013$) (Ref. 16) is found although it is nearly covered by background signal. These ESR results directly proved the existence of V_{Zn}^- and Cu^{2+} in the Cu-doped ZnO thin films. For the similar samples measured under the same conditions, the spin concentration can be approximately expressed by an equation: $N \propto A \bullet (\Delta H_{pp})^2$, where N is the spin concentration, A is the amplitude and ΔH_{pp} is width of the first derivative ESR spectrum. According to our ESR results, with the increase in P_O , the amplitude has a decrease trend while all the curves have the same ΔH_{pp} , which indicates the carrier concentration is reduced in thin films when prepared at high P_O . In addition, the gradually clear peak indicates the increase in density of V_{Zn}^- defects.

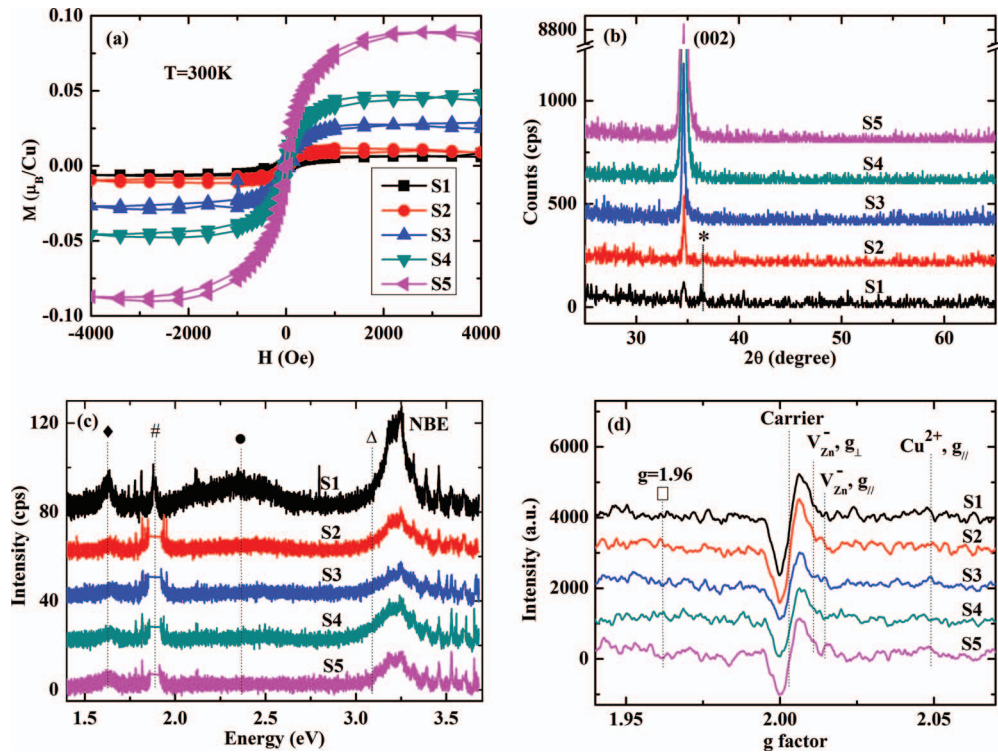


FIG. 1. Magnetic, structural and optical properties measurements of samples S1, S2, S3, S4 and S5 prepared at different P_O . (a) M - H curves measured at room temperature with the applied magnetic field parallel to the film surface. (b) XRD patterns and the symbol “*” represents ZnO (101) peak. (c) PL spectra and the symbol “♦”, “#”, “●” and “Δ” represent the red-emission peak, removed frequency-doubled laser, green-emission peak and UV-emission shoulder, respectively. (d) ESR spectra recorded at 270 K in a dark chamber and the symbol “□” represents the shallow donor state resonance peak.

The carrier concentration of Cu-doped ZnO thin films was estimated to be $<1.0 \times 10^{16} \text{ cm}^{-3}$ by a Hall Effect measurement system. The electron concentration is much lower than that of undoped ZnO thin films due to the formation of deep accept levels induced by Cu doping.¹⁷ It should be mentioned that the carrier concentration is lower than that in Mn-doped ZnO system reported by Dietl *et al.* (Ref. 18). Furthermore, the doped Cu concentration is about 3 at.%, which means the Bohr radius of Cu 3d wave function is not large enough to overlap with each other. Therefore, the RKKY theory which is focused on carrier-mediated exchange is unlikely responsible for the observed ferromagnetism in Cu-doped ZnO thin films. As discussed above, the XRD patterns, PL and ESR spectra give strong evidence for the existence of Cu^{2+} cation and V_{Zn} defect, thus it can be proposed that the observed ferromagnetism in poor conducting Cu-doped ZnO thin films is mediated by intrinsic point defects.

Herng *et al.* (Ref. 19) suggested an indirect double-exchange model in Cu-doped ZnO system, wherein, the Cu impurities are connected via the V_O orbital and ferromagnetically aligned. Coey *et al.* (Ref. 20) proposed a model of indirect exchange via shallow donors (V_O and/or Zn_i) for diluted ferromagnetic oxides and nitrides. These models are mainly focused on the shallow donors (V_O and Zn_i), however, the deep acceptor (V_{Zn}) is rarely considered. For the case of deep acceptor, the interaction is much more complicated compared to that in the former models, for which the valence band is degenerated.²¹ A possible mechanism is proposed and shown in Figure 2, where the ferromagnetism is mediated by ionized V_{Zn} . The Cu^{2+} with an outer shell electronic configuration of $3d^9$ has a spin angular momentum of 1/2, while the V_{Zn}^0 and V_{Zn}^- have spin angular momentum of 1 and 1/2, respectively. Three types of exchange interaction between spin polarized ions (Cu^{2+} cations and ionized V_{Zn}) are proposed. The neighboring Cu^{2+} ions (left bottom corner) within $\sim \text{\AA}$ distance will favor anti-ferromagnetic interaction. Ferromagnetic interaction between Cu^{2+} cations and ionized V_{Zn} can be explained by RKKY theory (Ref. 18). The ferromagnetic interaction between

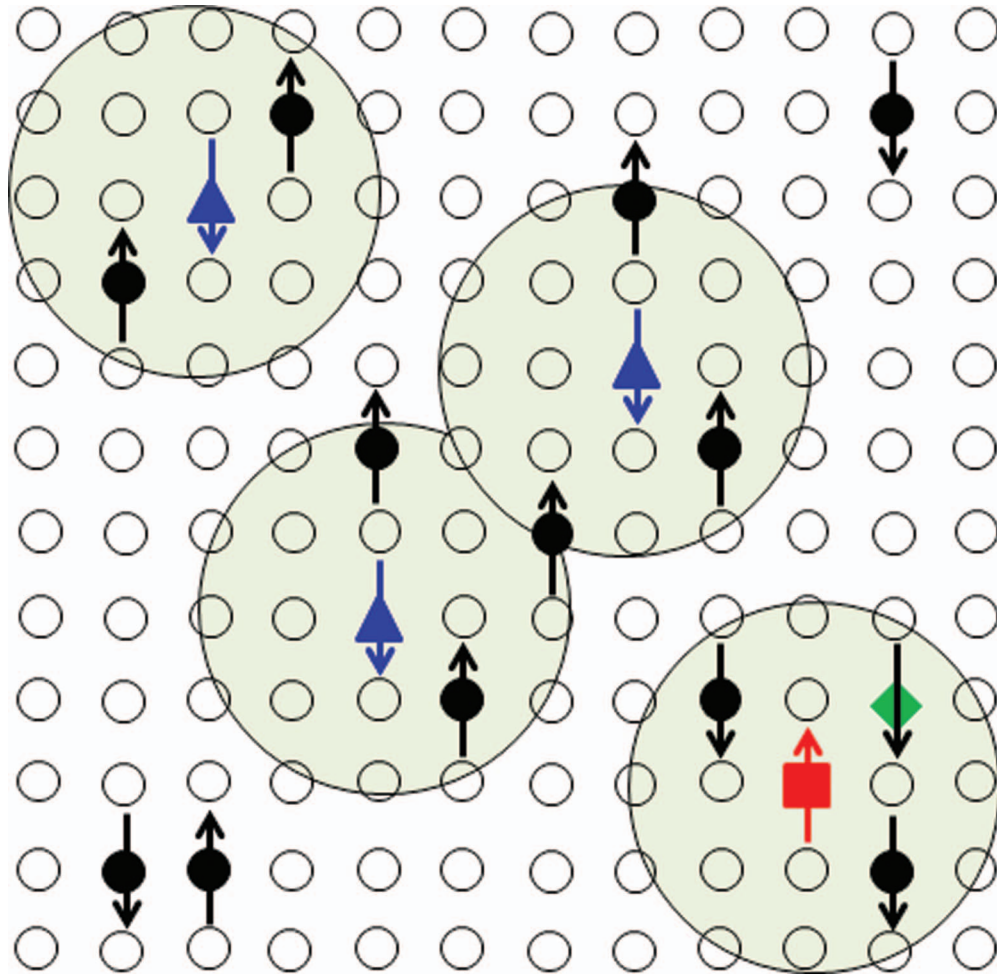


FIG. 2. Schematic diagram of ferromagnetic mechanism for ionized V_{Zn} embedded in Cu-doped ZnO system. White circles, black circles, green rhombus, blue triangles, red square and large olive circles represent zinc atoms, Cu^{2+} cations, Cu^{3+} cations, neutral V_{Zn}^0 defects, ionized V_{Zn}^- defect and interaction range of ionized zinc vacancy, respectively. Oxygen atoms are not shown here.

ionized V_{Zn} is complicated and still unclear now. As shown in Figure 2, isolated Cu^{2+} , V_{Zn}^0 and V_{Zn}^- show random spin orientations. When considering the exchange interaction between the spin polarized ions, ionized V_{Zn} tends to form bound magnetic polarons and coupled the Cu^{2+} cations within their orbits. The adjacent bound magnetic polarons can overlap with each other and make all the Cu^{2+} cations parallel to a uniform orientation. It is noteworthy that Cu^{3+} ions with $s = 1$ should be considered in this zinc vacancy rich system. Kataoka *et al.* (Ref. 22) observed a clear Cu $2p \rightarrow 3d$ signal in Cu doped ZnO nanowire by x-ray magnetic circular dichroism, which indicates a small amount of Cu^{2+}/Cu^{3+} states in the bulk region is magnetically active. Extra holes from zinc vacancies would transfer into Cu $3d$ orbitals and form Cu^{3+} cations. The Cu^{3+} cations were mediated by zinc vacancies and parallel aligned to each other, making contribution to the ferromagnetism of the Cu-doped ZnO thin films. Furthermore, it is interesting to note that the saturation magnetization in this paper ($\sim 0.1 \mu_B/Cu$) is smaller than the calculated value ($1 \mu_B/Cu$) (Ref. 23), which can be easily explained from figure 2. The isolated Cu^{2+} cations and un-interacted ionized V_{Zn} will not contribute to the ferromagnetism. In addition, copper atoms occupying adjacent cation lattice positions will result in anti-ferromagnetic alignment, which also will reduce the saturation magnetization.

In conclusion, ferromagnetic Cu-doped ZnO thin films with nominal concentration of 3 at.% were prepared by an ICP-PVD system at different P_O . SQUID measurements indicate that the

saturation magnetization increases with improving the P_O . The XRD and ESR results present the evidence of Cu^{2+} cations. PL and ESR measurements indicate the existence of ionized V_{Zn} in all the thin films, and a subtle enhancement of ionized V_{Zn} signal is observed with increasing the P_O . A quasi-indirect exchange model has been tentatively proposed for the Cu-doped ZnO thin films, where the ferromagnetism is mediated by ionized V_{Zn} .

ACKNOWLEDGMENTS

This work is supported by the Young Scientists Fund of the National Natural Science Foundation of China (Grant no. 51002176) and the Innovation Program of the Shanghai Institute of Ceramics.

- ¹ K. Sato and H. Katayama-Yoshida, *Jpn. J. Appl. Phys. Part 2-Letters* **39**, L555 (2000).
- ² Z. A. Khan and S. Ghosh, *Appl. Phys. Lett.* **99**, 042504 (2011).
- ³ H. S. Hsu, J. C. A. Huang, Y. H. Huang, Y. F. Liao, M. Z. Lin, C. H. Lee, J. F. Lee, S. F. Chen, L. Y. Lai, and C. P. Liu, *Appl. Phys. Lett.* **88**, 242507 (2006).
- ⁴ L. H. Ye, A. J. Freeman, and B. Delley, *Phys. Rev. B* **73**, 033203 (2006).
- ⁵ Y. M. Hu, S. S. Li, and C. H. Chia, *Appl. Phys. Lett.* **98**, 052503 (2011).
- ⁶ H. Liu, X. Zhang, L. Li, Y. X. Wang, K. H. Gao, Z. Q. Li, R. K. Zheng, S. P. Ringer, B. Zhang, and X. X. Zhang, *Appl. Phys. Lett.* **91**, 072511 (2007).
- ⁷ L. S. Vlasenko and G. D. Watkins, *Phys. Rev. B* **72**, 035203 (2005).
- ⁸ D. B. Buchholz, R. P. H. Chang, J. H. Song, and J. B. Ketterson, *Appl. Phys. Lett.* **87**, 082504 (2005).
- ⁹ S.-Y. Zhuo, X.-C. Liu, Z. Xiong, J.-H. Yang, and E.-W. Shi, *J. Cryst. Growth* **332**, 39 (2011).
- ¹⁰ R. Elilarassi, P. S. Rao, and G. Chandrasekaran, *J. Sol-Gel Technol.* **57**, 101 (2011).
- ¹¹ C. H. Ahn, Y. Y. Kim, D. C. Kim, S. K. Mohanta, and H. K. Cho, *J. Appl. Phys.* **105**, 013502 (2009).
- ¹² B. X. Lin, Z. X. Fu, and Y. B. Jia, *Appl. Phys. Lett.* **79**, 943 (2001).
- ¹³ Y. Fang, Y. Wang, Y. Wan, Z. Wang, and J. Sha, *J. Phys. Chem. C* **114**, 12469 (2010).
- ¹⁴ A. J. Reddy, M. K. Kokila, H. Nagabhushana, R. P. S. Chakradhar, C. Shivakumara, J. L. Rao, and B. M. Nagabhushana, *J. Alloys Compd.* **509**, 5349 (2011).
- ¹⁵ S. Moribe, T. Ikoma, K. Akiyama, Q. Zhang, F. Saito, and S. Tero-Kubota, *Chem. Phys. Lett.* **436**, 373 (2007).
- ¹⁶ M. Kakazey, M. Vlasova, M. Dominguez-Patino, G. Dominguez-Patino, T. Sreckovic, and N. Nikolic, *Sci. Sinter.* **36**, 65 (2004).
- ¹⁷ H. J. Lee, B. S. Kim, C. R. Cho, and S. Y. Jeong, *Phys. Status Solidi B* **241**, 1533 (2004).
- ¹⁸ T. Dietl, H. Ohno, F. Matsukura, J. Cibert, and D. Ferrand, *Science* **287**, 1019 (2000).
- ¹⁹ T. S. Herg, D. C. Qi, T. Berlijn, J. B. Yi, K. S. Yang, Y. Dai, Y. P. Feng, I. Santoso, C. Sanchez-Hanke, X. Y. Gao, A. T. S. Wee, W. Ku, J. Ding, and A. Rusydi, *Phys. Rev. Lett.* **105**, 207201 (2010).
- ²⁰ J. M. D. Coey, M. Venkatesan, and C. B. Fitzgerald, *Nat. Mater.* **4**, 173 (2005).
- ²¹ A. C. Durst, R. N. Bhatt, and P. A. Wolff, *Phys. Rev. B* **65**, 235205 (2002).
- ²² T. Kataoka, Y. Yamazaki, V. R. Singh, A. Fujimori, F. H. Chang, H. J. Lin, D. J. Huang, C. T. Chen, G. Z. Xing, J. W. Seo, C. Panagopoulos, and T. Wu, *Phys. Rev. B* **84**, 153203 (2011).
- ²³ G. Shukla, *Appl. Phys. A* **97**, 115 (2009).